SC 1004-A (2-54)

[redacted]

UNCLASSIFIED

CLASSIFIED LIBRARY
Ref. Sym: ~~5141 (975)~~

94

C-159

[redacted]

[redacted]

SC-TM-129-55-51

# THE STABILITY OF FIN-STABILIZED, LOW-FINENESS-RATIO BODIES OF REVOLUTION

SANDIA SYSTEMS
1st Review Date: 1-28-80
Authority: LIADC
Name: CCRP-RR
2nd Review Date: 12-10-96
Authority: ADD
Name: W Logue
Classification Changed to: U
Classification Changed to: U
Classification Changed to: U
Classified with
Classified UCAI?
Comments: Unclassified

Paul W. Rowe

SANDIA SYSTEMS
DOE
CLASSIFICATION CHANGED TO: U
Emilda Selph
PERSON CHANGING MARKING & DATE
R. T. Duff
PERSON VERIFYING MARKING & DATE
AUTHORITY: CCRP-RR
RECORD ID: 97SN126
DATED: 12/10/96

ABSTRACT

A method is developed which allows computation of the longitudinal stability of low-fineness-ratio, fin-stabilized bodies of revolution. Computed stability characteristics are shown to agree comparatively well with characteristics obtained from wind-tunnel tests. In addition, the analysis developed indicates possible causes of the unusual stability characteristics typical of low-fineness-ratio shapes and suggests possible ways in which the analysis may be refined.

[redacted]

[redacted]

INVENTORIED
DATE 3-22-64

Case No. 409.04

UNCLASSIFIED

June 30, 19[illegible]

1100/142

[redacted]

UNCLASSIFIED

DISTRIBUTION:
Dr. Paul Lieber, P. O. Box 841, Troy, New York
G. E. Hansche, 5140
A. Y. Pope, 5142
O. L. Bashor, 1242-1 [redacted]
R. K. Smeltzer, 1922-2
M. K. Linn, 1923 (6)

UNCLASSIFIED

[redacted]

UNCLASSIFIED

# THE STABILITY OF FIN-STABILIZED, LOW-FINENESS-RATIO BODIES OF REVOLUTION

## INTRODUCTION

The design of aeroballistic shapes is often a compromise between the desires of the aerodynamicist and limitations imposed by unavoidable practical requirements. As a consequence, aeroballistic shapes have been known to evolve which possess geometric characteristics more akin to barrels or eggs than to the more ideal, highly streamlined bodies. No matter what the shape of the body, the aerodynamicist is obligated to insure that the configuration will exhibit the desired aerodynamic characteristics. If the shape is restricted by practical limitations to be barrel or egg-like, the task of providing the desired aerodynamic characteristics is not always simple, particularly if the operating Mach numbers of the configuration include the region about a Mach number of unity.

For many applications requiring the use of barrel-like shapes, the configuration must be statically and dynamically stable. Many of these applications may eliminate the use of spin to provide stabilization and, at the same time, limit the size of stabilizing surface (fin surface) that can be used to provide the required stability characteristics. As a consequence of the barrel or egg-like shape and restrictions placed upon stabilizing surface, definition of an acceptable configuration is not self-evident a priori. This lamentable situation could be improved if there existed methods for predicting the aerodynamic characteristics of these low-fineness-ratio shapes. Unfortunately no such methods are available for shapes of this sort although methods do exist for bodies of high-fineness-ratio. This anomaly exists for reasons which are quite fundamental: high-fineness-ratio shapes are usually preferred for most applications where limitations do not prevent their use, and equations of motion of a compressible fluid flow about a body can be greatly simplified (and usually solved) for a body whose length is large compared to its diameter. This simplification cannot be made for low-fineness-ratio shapes, however, and solution of the equations of motion are the exception rather than the rule.

Although exact solutions of the equations of motion of compressible fluid flow about low-fineness-ratio shapes cannot be expected, it is hoped that approximate analytical methods can be developed which will predict the aerodynamic characteristics of these shapes. It is the purpose of this memorandum to discuss this possiblity and to present one crude method of determining some of the stability characteristics of these shapes. To prevent this memorandum from becoming too voluminous, the discussion is generally limited to the stability of a fin-stabilized, low-fineness-ratio body of revolution with one degree of freedom, i.e., rotation about a lateral axis through the center of gravity. For purposes of this memorandum, low-fineness-ratio is taken to mean fineness ratios in the range 2 to 5.

## NOTATION*

$a$ - Local body radius, ft

$\bar{a}$ - Mean radius of that portion of the afterbody located between the leading and trailing edge of the fin, ft

$B_b$ - Body base area, sq ft

$B_m$ - Mean cross-sectional area of body, sq ft

* See also Figure 1.

UNCLASSIFIED

[redacted]

UNCLASSIFIED

$B_n$ - Area of body nose flat, sq ft

b - Fin semispan, ft

$C_L$ - Lift coefficient, $(2\ L/\rho V^2 S)$

$C_{L_\alpha}$ - Change of lift coefficient with angle of attack, $(\partial C_L/\partial \alpha)$, per degree

$C_m$ - Pitching moment coefficient, $(2M/\rho V^2 Sd)$

$C_{m_\alpha}$ - Change of pitching moment coefficient with angle of attack, $(\partial C_m/\partial \alpha)$, per degree

$\left[-C_{m_\alpha}\right]$ - Static stability coefficient. Body is statically stable if value of this bracketed coefficient is positive, unstable if the value is negative. Degree of stability or instability is indicated by the magnitude of this coefficient.

$C_{m_{\dot{\alpha}}}$ - Change of moment coefficient with rate change of angle of attack, $\left[\dfrac{\partial C_m}{\partial\left(\frac{\dot{\alpha} d}{2V}\right)}\right]$ per radian

$C_{m_q}$ - Change of moment coefficient with pitching velocity, $\left[\dfrac{\partial C_m}{\partial\left(\frac{qd}{2V}\right)}\right]$, per radian

$\left[-\left(C_{m_q} + C_{m_{\dot{\alpha}}}\right)\right]$ - Dynamic stability parameter. Body is dynamically stable if value of this bracketed parameter is positive, unstable if the value is negative. Degree of stability or instability is indicated by the magnitude of this coefficient.

d - Maximum diameter of body not including surface perturbations, ft

L - Lift force, lbs

$\ell$ - Total body length, ft

$\ell_a$ - Length of afterbody between leading and trailing edge of the fins, ft

$\ell_t$ - Distance from center of pressure of the fin to body center of gravity, ft

$\ell_{ta}$ - Distance from center of pressure of the afterbody to body center of gravity, ft

M - Pitching moment about body center of gravity; has a positive value if moment tends to increase the nose-up angle of attack, ft-lbs

p - Local static pressure, psf

$p_a$ - Ambient, or free stream pressure, psf

$\Delta p$ - Local pressure differential between upper and lower symmetrically opposed surface points.

UNCLASSIFIED

$q$ - Pitching velocity about center of gravity, radians/sec

$r$ - Distance of a point from the longitudinal body axis, $(r^2 = y^2 + z^2)$, ft

$S$ - Major body cross-sectional area, $(\pi d^2/4)$, sq ft

$S_t$ - Total effective area of tail fin, sq ft

$t$ - Time, sec

$V$ - Total velocity of body relative to air stream, fps

$U$ - Component of velocity normal to longitudinal axis of the body, fps

$x$ - Longitudinal coordinate, ft

$x_o$ - Distance from nose to center of gravity of the body, ft

$\bar{x}$ - Distance of centroid of body volume from the nose, $\left(\frac{\int_0^l \pi a^2 \, x dx}{B_m l}\right)$, ft

$y$ - Lateral coordinate, ft

$z$ - Vertical coordinate, ft

$x,y,z$ - Rectangular coordinate body axes as noted above and illustrated in Fig. 1

$\alpha$ - Angle of attack of the body, degrees

$\alpha_a$ - Local angle of attack at the afterbody, degrees

$\alpha_t$ - Local angle of attack at the tail fin, degrees

$\dot{\alpha}$ - Rate change of angle of attack, $(\partial\alpha/\partial t)$, rad. per sec

$\epsilon$ - Average downwash angle over the tail fin, degrees

$\epsilon_1$ - Local downwash angle at root chord of the tail fin, degrees

$\epsilon_2$ - Local downwash angle at tip chord of the tail fin, degrees

$\theta$ - Angular orientation of a point in the (y, z) plane, see Fig. 1

$\phi$ - Velocity potential, $ft^2/sec$

$\rho$ - Free-stream density, $slugs/ft^3$

Subscripts

$]_b$ - Body

$]_t$ - Fin

$]_a$ - Afterbody

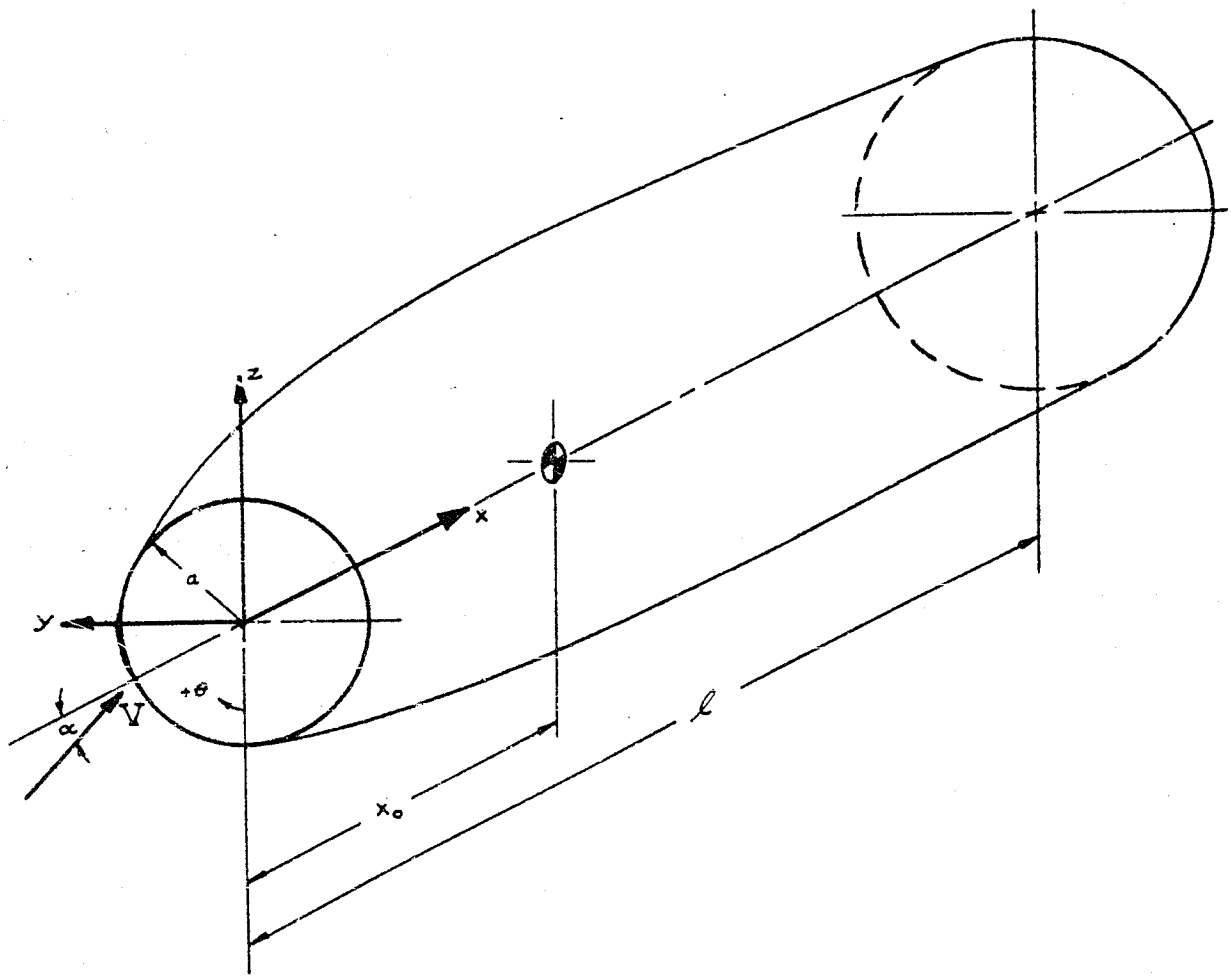


Fig. 1 - Body Coordinate System

## PRESENT STATE OF KNOWLEDGE

The present "state-of-knowledge" of the stability characteristics of low-fineness-ratio bodies derives largely from observations of wind-tunnel tests. A great mass of data is available from these tests, a portion of which can lead to some general conclusions and rules of thumb regarding the stability characteristics typical of low-fineness-ratio bodies. Without becoming too specific, the following observations are generally true:

1. There appears to be a kind of "conservation of stability", i.e., an increase of static stability is usually accompanied by a decrease of dynamic stability for any given configuration.

2. Stability seems to be a sensitive function of nose shape, and increasing the nose flat diameter will usually increase the static stability at the expense of dynamic stability.

3. "Clean" low-fineness-ratio bodies will usually exhibit a region of dynamic or static instability which may be remedied by adroit application of circumferential spoiler bands.

4. Stability parameters of low-fineness-ratio shapes exhibit tendencies to be nonlinear functions of angle of attack.

The causes of the above phenomena are not readily apparent. However, it does appear possible to at least partially explain certain of the above observations by analyzing, in a crude way, the stability of low-fineness-ratio bodies. Furthermore, this crude analysis suggests more refined methods of attack, which, with suitable experimental verification, may lead to methods of predicting the desired stability characteristics.

ANALYSIS

In the analysis of the stability characteristics of low-fineness-ratio bodies of revolution presented herein, only the static and dynamic stability parameters defined in the notation shall be discussed. These parameters arise in the course of examining the stability of a body free to rotate only about a lateral axis through the center of gravity and allowing no freedom of lateral or longitudinal motion.

In the form of preliminary remarks, it is assumed that the stability of a body is determined by the contribution to the stability of: the body alone, the fins, and the interference of the body on the fins and the fins on the body. As such, if each of these contributions can be determined and summed, the result should be the stability of the total configuration. Such a scheme shall be pursued.

Stability Contributions of the Body Alone

Mentioned previously was the nonexistence of solutions of the equations of motion governing the flow of a compressible fluid about a low-fineness-ratio body of revolution. Approximate solutions do exist, however, for bodies of high-fineness-ratio, and these solutions should provide a crude approximation at least, for the "fat" body. One method appearing to yield correct order of magnitude results for low-fineness-ratio bodies has been reported by Curry*. This method is based upon assumptions which allow very simple computation of the stability parameters for a body of revolution. These assumptions state that the body is of large-fineness-ratio; that the flow normal to the longitudinal axis (of symmetry) is incompressible; that the flow in a plane normal to the axis of symmetry is independent of the flow in adjacent planes; and that the body is performing slow oscillations about zero angle of attack. On the basis of these assumptions, the velocity potential for the body moving in the negative $z$ direction with a velocity, $U$,

$$\phi = \frac{U a^2 z}{y^2 + z^2} \tag{1}$$

which can be easily recognized as the flow potential for a doublet moving into a stream at rest with the axis of the doublet parallel to the $z$ axis of the body. The pressure differential between symmetrical points, $[(y_q + z), (y_q - z)]$, on the "upper" and "lower" surface of the body can be written:

$$\Delta p = 2\rho \left( \frac{\partial \phi}{\partial t} + V \frac{\partial \phi}{\partial x} \right) \tag{2}$$

Now for a body performing oscillations in the pitch plane, the vertical component of velocity, $U$, at any longitudinal station is given by:

$$U = V \sin \alpha + q(x - x_o), \text{ or}$$

$$U = V\alpha + q(x - x_o) \tag{3}$$

* Curry, W. H., "A Calculation of Mk 6 and Mk 5 Dynamic Stability", Sandia Corp. Ref. Sym: 5141-(375), CRD.

since the angle of attack shall be limited to the region wherein

$$\sin \alpha \cong \alpha.$$

Substitution of Eq. (3) into (1), and the result into Eq. (2) yields an expression which may be integrated over the body to obtain the moments resulting from $\alpha$, $\dot{\alpha}$, and $q$. When reduced to coefficient form, these relations become*:

$$-C_{m_\alpha}\Big]_b = \frac{2\left[B_b(\ell - x_o) + B_n x_o - B_m \ell\right]}{57.3\ Sd} \tag{4}$$

$$-C_{m_q}\Big]_b = \frac{4\left[B_b(\ell - x_o)^2 - B_n x_o^2 - B_m \ell\ (\bar{x} - x_o)\right]}{Sd^2} \tag{5}$$

$$-C_{m_{\dot{\alpha}}}\Big]_b = \frac{4B_m \ell(\bar{x} - x_o)}{Sd^2} \tag{6}$$

$$-\left(C_{m_q} + C_{m_{\dot{\alpha}}}\right)\Big]_b = 4\left[\frac{B_b(\ell - x_o)^2 - B_n x_o^2}{Sd^2}\right] \tag{7}$$

Equations (4) through (7) have some features worthy of note. First of all, they indicate that the body contribution to static stability will increase and that to dynamic stability decrease with increasing nose flat diameter if all other terms remain constant. Secondly, for a body with a given nose and base flat, the shape with least volume will possess the greater static stability, while the dynamic stability is independent of the shape of the body between the nose and base flat. Thirdly, these equations indicate that body possessing the shape of a right circular cylinder would possess neutral static stability ($C_{m_\alpha} = 0$) for any center of gravity location, but would be dynamically stable if the center of gravity were forward of the center of volume.

Unfortunately, very little body alone stability data is available with which to compare values predicted by these expressions. However, it is known** that a right circular cylinder does

---

* The expression for the body contribution to static stability does not appear in the paper by Curry.

**"Stability Characteristics of Single and Dual Right Circular Cylinders", by E. T. Clark, Sandia Corporation, Ref. Sym: 5141 (572).

[redacted]

UNCLASSIFIED

exhibit a degree of static stability for certain ranges of fineness ratio and center-of-gravity location. Some finned low-fineness-ratio shapes have indicated an increase of static stability and a decrease of dynamic stability with an increase of nose flat diameter, but whether this is due only to a change in the body contribution to stability is not known.

## Stability Contribution of the Fin plus Effect of Interference of the Body on the Fin Contribution

Since it is quite simple to include the effect of interference of the body on the fin stability contribution, the expressions derived in this section will include both. The moment about the center of gravity contributed by the fin for any given configuration angle of attack, $\alpha$, may be written as:

$$M]_t = - C_{L_{\alpha_t}}\Big]_t \alpha_t \frac{\rho}{2} V^2 S_t \ell_t \tag{8}$$

Now, if the body did not affect the fin contribution, the angle of attack of the fin, $\alpha_t$, would be identically equal to the angle of attack of the body, $\alpha$; and the lift curve slope of the fin would be the same whether or not it were mounted on the body. Since the body produces a local flow field by virtue of its presence, $\alpha_t$ is not equal to $\alpha$, and $C_{L_\alpha}]_t$ is not the same for the fin on the body and off the body. Let us first examine the effect of the body on the angle of attack of the tail. We have seen from the previous section that a body at some angle of attack, $\alpha$, gives rise to a cross flow velocity potential due to the cross flow velocity component $U = \alpha V$. If the body is assumed stationary, the cross flow velocity potential becomes, in cylindrical coordinates:

$$\phi = - U\left(r + \frac{a^2}{r}\right) \cos \theta \tag{9}$$

where

$$r = y^2 + z^2$$
$$r \cos \theta = - z$$

If the fins are assumed to be mounted at $\theta = 0$, $90^\circ$, $180^\circ$ and $270^\circ$ around the surface, then the fins at $90^\circ$ and $270^\circ$ are the only ones contributing to the stability. Eq. (9) can be used to determine the velocity at $\theta = 90^\circ$ and $270^\circ$ arising from the presence of the body. This velocity, $w$, is

$$w = U\left(1 + \frac{a^2}{r^2}\right) \tag{10}$$

Assuming the longitudinal velocity $V \cos \alpha = V$ is not affected by the presence of the body (this assumes a high-fineness-ratio shape) the local angle of attack, $\alpha_\ell$, becomes

$$\alpha_\ell = \frac{w}{V} \tag{11}$$

[redacted]



UNCLASSIFIED

[redacted]

UNCLASSIFIED

since

$$U = Va$$

the local angle of attack may be written

$$a_\ell = a\left(1 + \frac{a^2}{r^2}\right) \tag{12}$$

which becomes at the surface of the body (a = r)

$$a_\ell \Big]_{r = a} = \frac{2U}{V} = 2a \tag{13}$$

as indicated in Fig. 2(a).

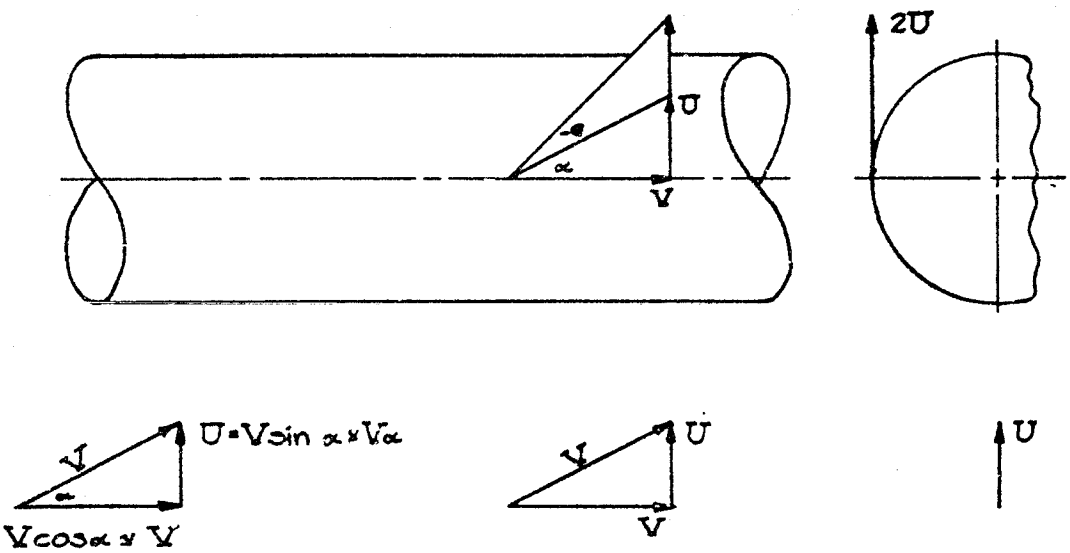


(a) Ideal Case

Fig. 2a - Illustration of Downwash

[redacted]

UNCLASSIFIED

If the difference between the local and body angle of attack be defined as the negative of the local downwash angle, $-\epsilon_\ell$,

$$-\epsilon_\ell = \alpha_\ell - \alpha$$

or

$$\alpha_\ell = \alpha - \epsilon_\ell \tag{14}$$

For the ideal case under consideration, comparison of Eqs. (14) and (12) shows that

$$-\epsilon_\ell = \alpha \frac{a^2}{r^2} \tag{15}$$

Assuming that the tail fin does not interfere with the flow around the body (more exactly, does not change the value of the local angle of attack as discussed above), then the angle of attack at the tail, for the ideal case, is

$$\alpha_t = \alpha - \epsilon \tag{16}$$

where $\epsilon$ is given approximately by

$$\epsilon = \frac{\epsilon_1 + \epsilon_2}{2} \tag{17}$$

and from Eq. (15)

$$\left.\begin{aligned} \epsilon_1 &= -\alpha \\ \epsilon_2 &= -\frac{\alpha a^2}{b^2} \end{aligned}\right\} \tag{18}$$

so that

$$\epsilon = -\frac{\alpha}{2}\left(1 + \frac{a^2}{b^2}\right) \tag{19}$$

and

$$\alpha_t = \alpha\left[1 + \frac{1}{2}\left(1 + \frac{a^2}{b^2}\right)\right] \tag{20}$$

The ideal case considered above is not quite typical of what is encountered in actual practice. The ideal case assumptions required instantaneous flow establishment to the potential given by Eq. (9), and divorced flow in adjacent laminates perpendicular to the axis of symmetry. Nor did it consider the possibilities of the presence of the fin causing variations in the cross flow. As a consequence, actual values of the downwash and local flow velocity are expected to be different from values given by Eqs. (10) and (15). This has been illustrated in Fig. 2(b).

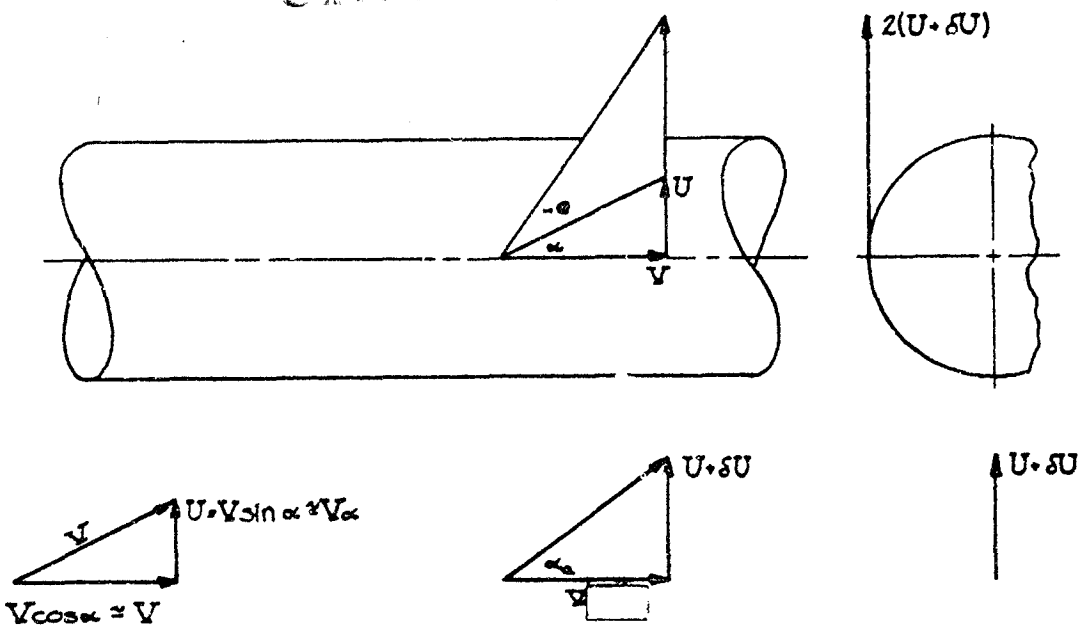


(b) Nonideal Case

Fig. 2b - Illustration of Downwash

However, Eq. (16) is general, since it amounts to a definition, and only needs the supplying of correct values of $\epsilon$. In the actual case, where the configuration is oscillating, $\epsilon$ may also not assume its "static" value immediately, but be subject to some lag. Consequently, if one includes the actual value of $\epsilon$ and the fin angle of attack due to a pitching velocity, $q\ell_t/V$, the angle of attack at the tail may be written:

$$\alpha_t = \alpha - \epsilon + \frac{q\ell_t}{V} \tag{21}$$

where

$$\epsilon = \frac{d\epsilon}{d\alpha}\left(\alpha - \frac{d\alpha}{dt}\,dt\right) \tag{22}$$

The value of downwash in Eq. 22 is assumed proportional to $\alpha$, and the second term accounts for possible lag in the establishment of $\epsilon$ when the body is oscillating, the total amount of lag being $\dot{\alpha}dt$, or $\Delta\alpha$, i.e., the value of $\epsilon$ lags its static value at $\alpha$ by an amount $\Delta\alpha = \dot{\alpha}dt$. It is to be re-emphasized that no lag would occur for the ideal case considered here.

Regarding $C_{L_{\alpha_t}}\Big]_t$, it is to be noted that this coefficient is the variation of tail lift coefficient with tail angle of attack, and that its value should be determined with the fin on the body. If the fin is on the body it is to be pointed out that

$$C_{L_\alpha}\Big]_t \neq C_{L_{\alpha_t}}\Big]_t$$

by virtue of Eq. (21).

[redacted]

UNCLASSIFIED

Having noted the above effects of the body upon the tail stability contribution, it is possible to insert Eqs. (21) and (22) into Eq. (8), the result being

$$M]_t = - C_{L_{\alpha_t}}]_t \left[\alpha - \frac{d\epsilon}{d\alpha}\left(\alpha - \frac{d\alpha}{dt}\,dt\right) + \frac{q\ell_t}{V}\right] \frac{\rho}{2} V^2 S_t \ell_t \tag{23}$$

Now if the total flow over the body is the cause of downwash at the tail, and the total body flow effects be assumed concentrated and originating at the body center of gravity (this point of concentration more properly should be taken at the body center of pressure, but the error involved is usually small) then a change in $\epsilon$ at the tail (caused by a change in body angle of attack), originating at the assumed point of concentration, will occur at a time $\ell_t/V$ later than the time of origin. Thus, Eq. (23) may be rewritten:

$$M]_t = - C_{L_{\alpha_t}}]_t \left[\alpha - \frac{d\epsilon}{d\alpha}\left(\alpha - \frac{\dot{\alpha}\ell_t}{V}\right) + \frac{q\ell_t}{V}\right] \frac{\rho}{2} V^2 S_t \ell_t \tag{24}$$

The fin contributions to the stability parameters are easily obtained from Eq. (24) and are:

$$- C_{m_\alpha}]_t = C_{L_{\alpha_t}}]_t \frac{S_t}{S}\frac{\ell_t}{d}\left(1 - \frac{d\epsilon}{d\alpha}\right) \tag{25}$$

and

$$- \left(C_{m_q} + C_{m_{\dot{\alpha}}}\right)\Big]_t = 2C_{L_{\alpha_t}}]_t \frac{S_t}{S}\left(\frac{\ell_t}{d}\right)^2\left(1 + \frac{d\epsilon}{d\alpha}\right) \tag{26}$$

if $C_{L_{\alpha_t}}]_t$ is assumed constant with respect to $\alpha$, $\dot{\alpha}$, and $q$.

A comparison of Eqs. (25) and (26) indicates that a change in the value of $d\epsilon/d\alpha$ will affect the two parameters in an opposite sense, i.e., increase the value of one while decreasing the other. This indicates a possible explanation for the "conservation of stability" noted in the stability tests of low-fineness-ratio, fin-stabilized bodies. It is to be noted from Eq. (24) that if no lag in $d\epsilon/d\alpha$ exists, that the fins could provide no contribution tending toward dynamic instability since $d\epsilon/d\alpha$ would not appear in Eq. (26). It is also noted that $d\epsilon/d\alpha$ must be negative if the fins are to contribute to dynamic instability. Unfortunately, Eq. (19) indicates that $d\epsilon/d\alpha$ will be negative, at least in the ideal case, and there is no reason to hope for non-negative values in an actual situation.

We have achieved, at this point, analytical expressions for the contributions of the body, and fins plus body interference to the total stability of a configuration. It would be anticipated that the sum of these two would compose the predominant portion of body stability. Consequently, we shall digress at this point and compute the total stability as given by the sum of these two contributions. Since a large amount of stability data is available for the Mk 4 and Mk 6 shapes*,

* The visible differences in these shapes consist of five rows of circumferential spoiler bands added to the center portion of the Mk 6.

[redacted]

UNCLASSIFIED

the contributions of these shapes will be determined, summed, and compared with the stability parameters obtained from wind-tunnel tests.

Referring to Eqs. (4) and (7), it is seen that the body contribution is expressed as a function of body geometry only. For the Mk 4 and Mk 6, the appropriate shape constants are:

$B_b = 5.94 \text{ ft}^2$

$B_n = 4.58 \text{ ft}^2$

$S = 19.65 \text{ ft}^2$

$d = 5.00 \text{ ft}$

$\ell = 10.66 \text{ ft}$

$x_o = 3.33 \text{ ft}$ (c.g. at 40" full scale)

$B_m = 14.70 \text{ ft}^2$

Inserting these values into Eqs. (4) and (7) yields for the body contributions of the Mk 4 and Mk 6:

$$- C_{m_\alpha}\Big]_b = - 0.0347 \text{ per deg}$$

$$- \left(C_{m_q} + C_{m_{\dot\alpha}}\right)\Big]_b = 2.18 \text{ per rad.}$$

from which it is seen that the body alone is statically unstable but dynamically stable. Since the analytical expressions obtained for the body alone are incapable of differentiating between the Mk 4 and Mk 6 shapes, only the values shown can be computed for these bodies. The body alone values are also independent of Mach number as a result of the assumptions used to derive Eqs. (4) and (7).

The fin contribution can be determined from Eqs. (24) and (25) using the value of $\epsilon$ for the ideal case prescribed by Eq. (19) and assuming a value of $C_{L_{\alpha_t}}\Big]_t$ tempered by data on similar wing sections if these exist. Fortunately, measurements of $d\epsilon/d\alpha$ and $C_{L_{\alpha_t}}\Big]_t$ exist for the Mk 4 and Mk 6, and it appears more appropriate to use these experimental values than the theoretical ones.

Fin force measurements* on the Mk 4 and Mk 6 fins were made and allowed determination of $C_{L_\alpha}\Big]_t$. These values are presented in Fig. 3 as the topmost curves. From the discussion of this section it may be shown that

$$C_{L_{\alpha_t}}\Big]_t = \frac{C_{L_\alpha}\Big]_t}{1 - \frac{d\epsilon}{d\alpha}}$$

*Rice, M. A., "Fin Performance Tests of Sandia Mk 4 and Mk 6 Model", CAL report, 784-002-1, October 1953, CRD.

UNCLASSIFIED

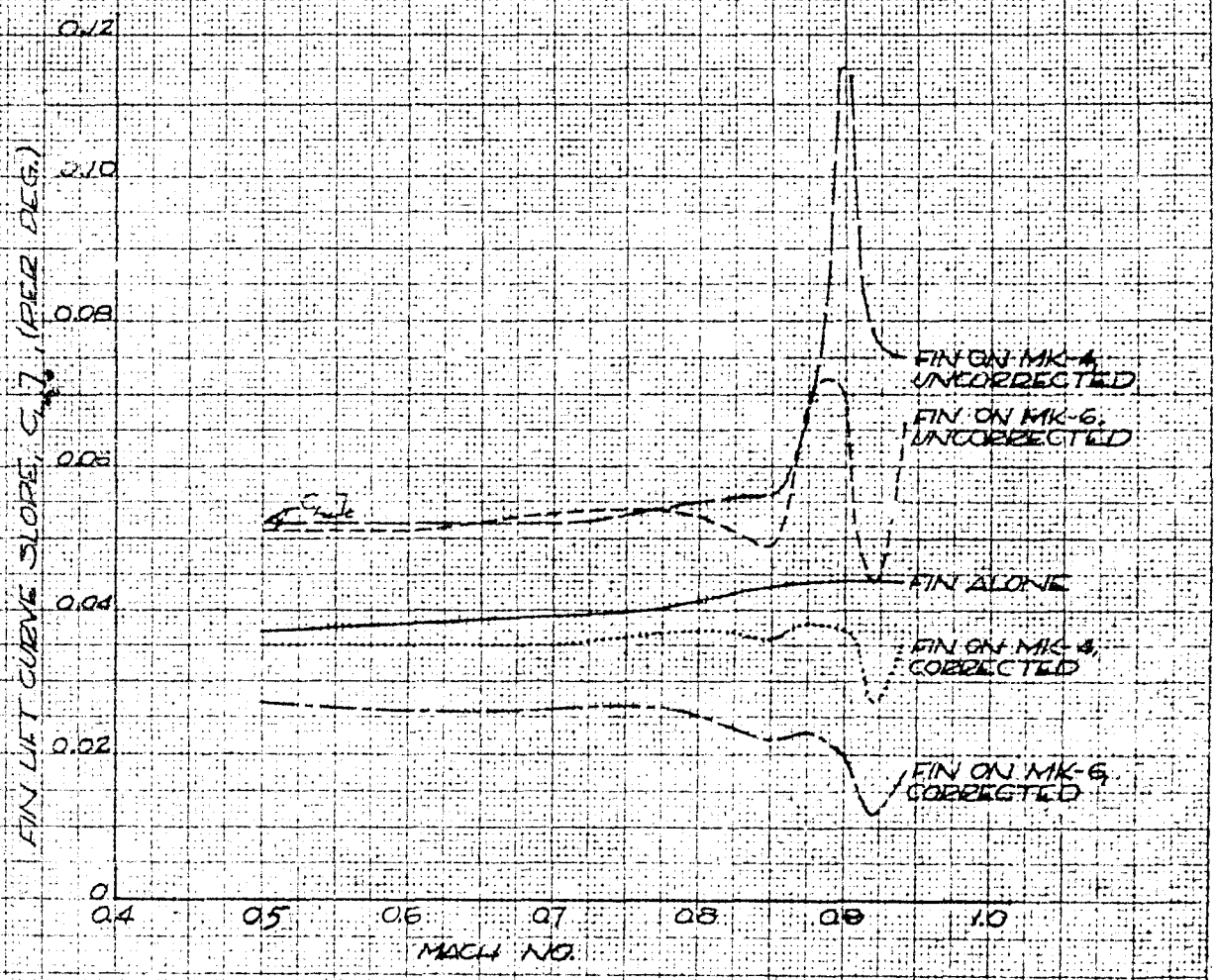


FIG. 3 - EFFECT OF BODY ON FIN LIFT CURVE SLOPE

UNCLASSIFIED



10 X 10 TO THE CM 359-14

[redacted]

UNCLASSIFIED

Values of $d\epsilon/d\alpha$ at the fin were determined from this program and were used to 'correct' the values of $C_{L_\alpha}]_t$ to obtain $C_{L_{\alpha_t}}]_t$. These values of $d\epsilon/d\alpha$ (taken as the slope of the variation of $\epsilon$ with $\alpha$ for the range $(-4^\circ < \alpha < 4^\circ)$) are plotted in Fig. 4, and values of $C_{L_{\alpha_t}}]_t$ in Fig. 3. The effect of the body on the fin lift curve slope is illustrated on Fig. 3 by comparing the lower two curves, obtained by the above process, with lift curve slopes obtained on the Mk 4 and Mk 6 fin measured without being mounted on the body.* It is noted from Fig. 3, that $C_{L_{\alpha_t}}]_t$ values for the fins mounted on the body are significantly lower than values obtained for the fins alone. This is surely to be expected since the fins when mounted on the body are partially submerged in the low velocity region surrounding the afterbody.** This region is considerably larger for the Mk 6 than for the Mk 4. The fin contributions to the stability parameters may now be computed from Eqs. (24) and (25) using the values of $d\epsilon/d\alpha$ presented in Fig. 4, the values of $C_{L_{\alpha_t}}]_t$ presented in Fig. 3, assuming the lag in downwash is equal to $\ell_t/V$, and using the following geometric characteristics of the fins:

$S_t = 8.80$ ft$^2$ (4.40 sq ft per fin)

$\ell_t = 5.22$ ft.

For this computation the fins were assumed to lie in a plane normal to the plane of pitch.*** The body and fin contributions computed for the Mk 4 and Mk 6 were summed and the results plotted in Figs. 5 through 8. Also included thereon are values of the stability parameters directly determined from dynamic-type wind-tunnel tests of these configurations. For both computed and experimental values, the center of gravity was at 40 inches full scale aft of the nose flat. These figures indicate that the computed sums are quite universally below values obtained from the wind-tunnel tests, the difference between the values determined in each manner being of appreciable magnitude. Comparison in a qualitative sense is observed to be reasonable, however.

In an effort to discover plausible explanations for the nonagreement between computed and experimental values, it seems logical to examine more closely the contributions of the various parts of the configuration. Because of the manner in which the fin contribution was determined, the fin contribution included the effects of the body on the fin contribution. As such, the fin contribution should be quite accurate if the lag value assumed is reasonable. Since computed values of both the static and dynamic stabilities were in error, revising the lag value assumed could only improve the dynamic stability agreement. On the other hand, accuracy of the body contribution as computed seemed unassessable, and from the coarseness of the assumptions used to evaluate the body theory, it appeared that the computed body contributions could be grossly different from values which might be obtained experimentally. The Mk 4 body-alone static stability parameter obtained in the wind tunnel**** has been plotted along with the computed value in Fig. 9. To Mach numbers of approximately 0.7, the comparison is no less than remarkable, and the computed values from the theory exhibit order of magnitude correctness for the entire Mach number range. Now if the computed fin contribution is added to the experimentally determined

---

* Unpublished report by R. C. Maydew, "CWT Wing Tunnel Test #287 - Reflection Plane Force Tests of Several Full Scale Fins".

** Maydew, R. C., "Analysis of Pressure Rake Studies of the Flow Field Over the Afterbody of the Mk 6 and TX-13 Wind Tunnel Models", Sandia Corporation Ref. Sym: 5141-(330), CSI.

*** In a program run at Cornell Aeronautical Laboratory (CAL 784-008) the Mk 6 exhibited no real stability differences with the fins at 45° to the plane of pitch or at 0° and 90° to the plane of pitch. Although the wind-tunnel data is usually obtained with the fins at 45°, the analytical procedure is simplified for the 90° orientation, and since no real difference was obtained experimentally, the 90° orientation was assumed for the computation.

**** Zebb, Keirn, "Report on High Speed Wind-Tunnel Test Series HA-1", CWT Report No. 74, 1949, SRD.

[redacted]

UNCLASSIFIED

[redacted]

UNCLASSIFIED

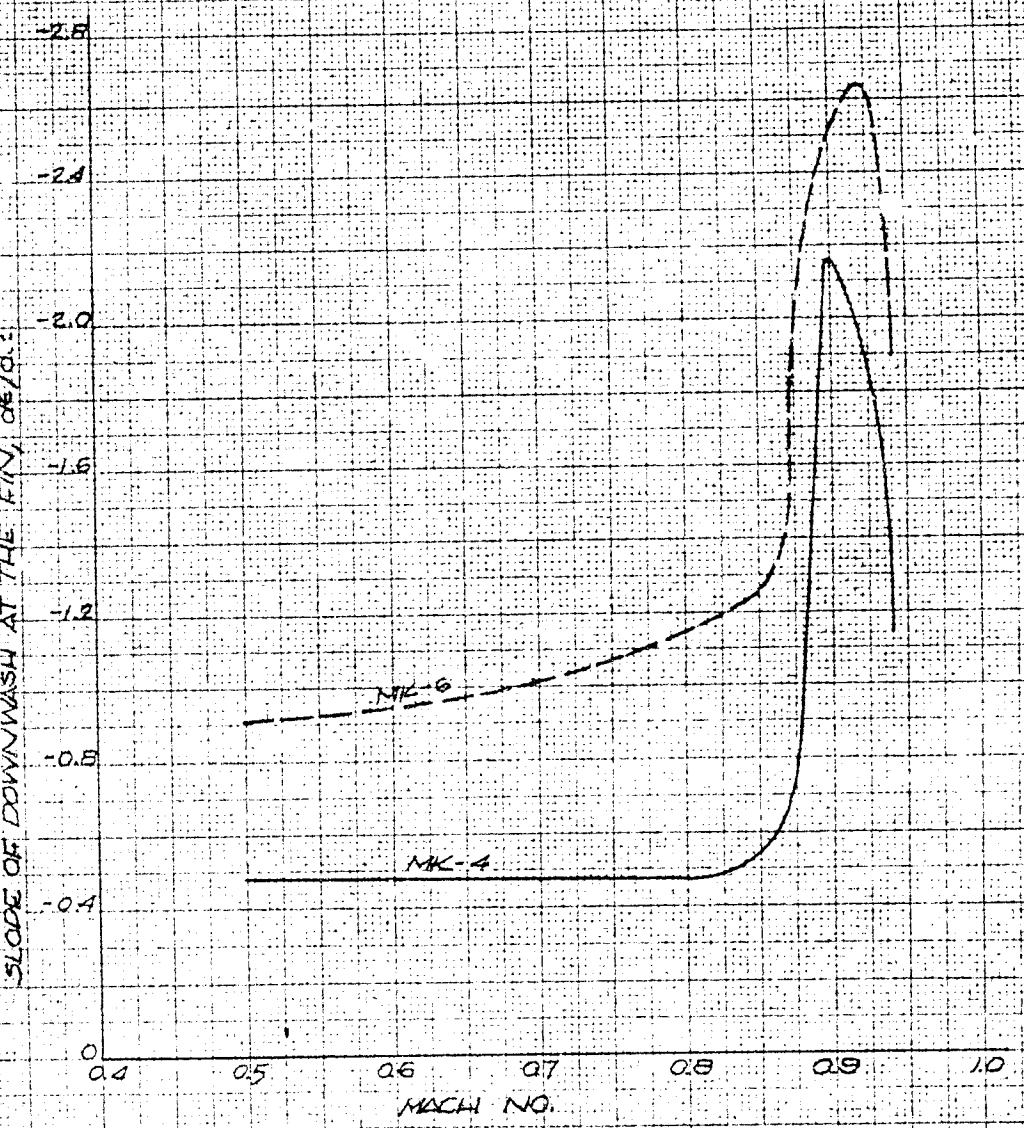


FIG 4 - VARIATION OF dε/dα WITH MACH NUMBER

[redacted]

UNCLASSIFIED

PREP. BY _____ DATE _____

10 X 10 TO THE CM. 359-14

[redacted]

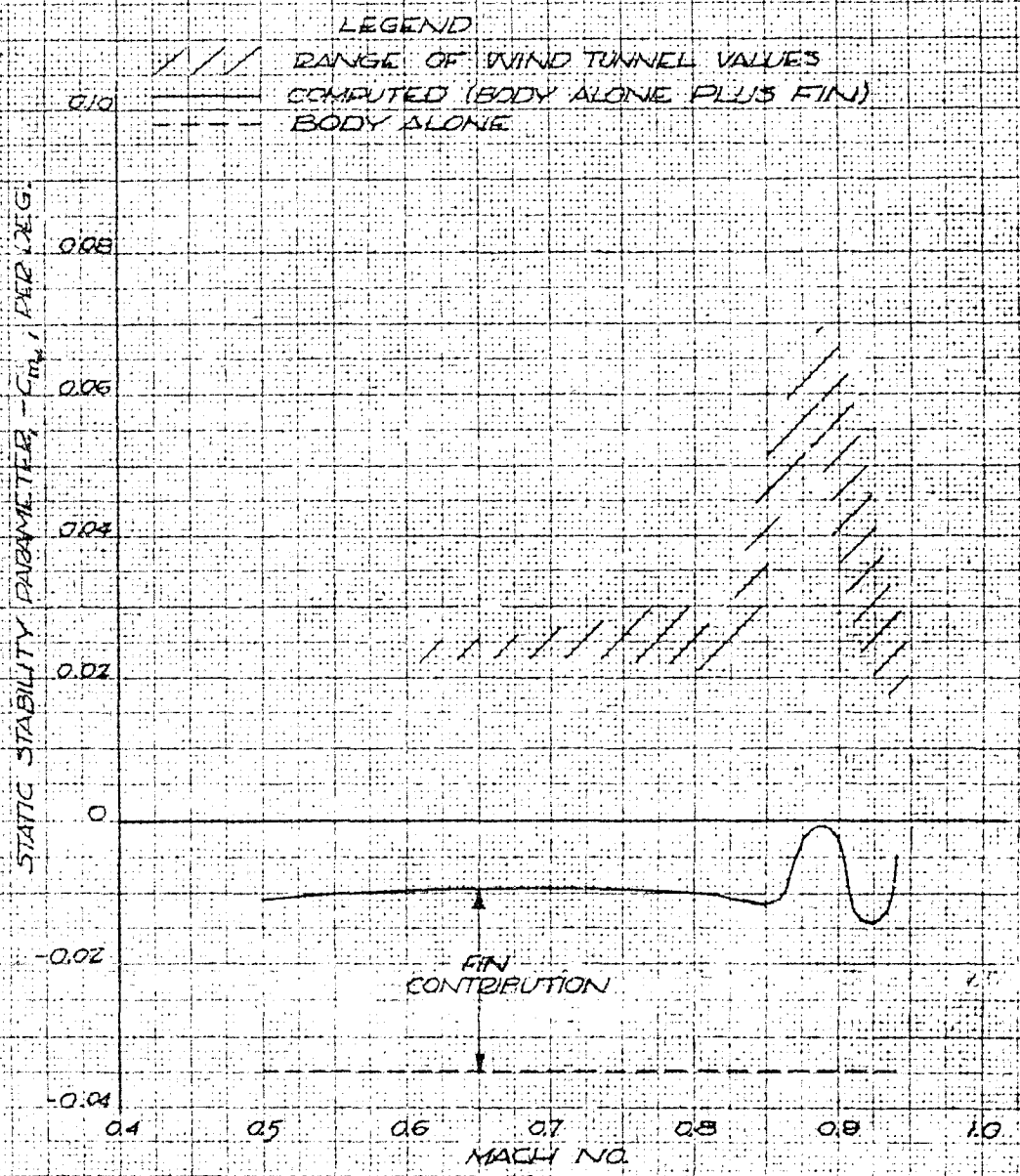


FIG 5 - COMPARISON OF MK-6 STATIC STABILITY PARAMETERS

[redacted]



UNCLASSIFIED

[redacted]

UNCLASSIFIED

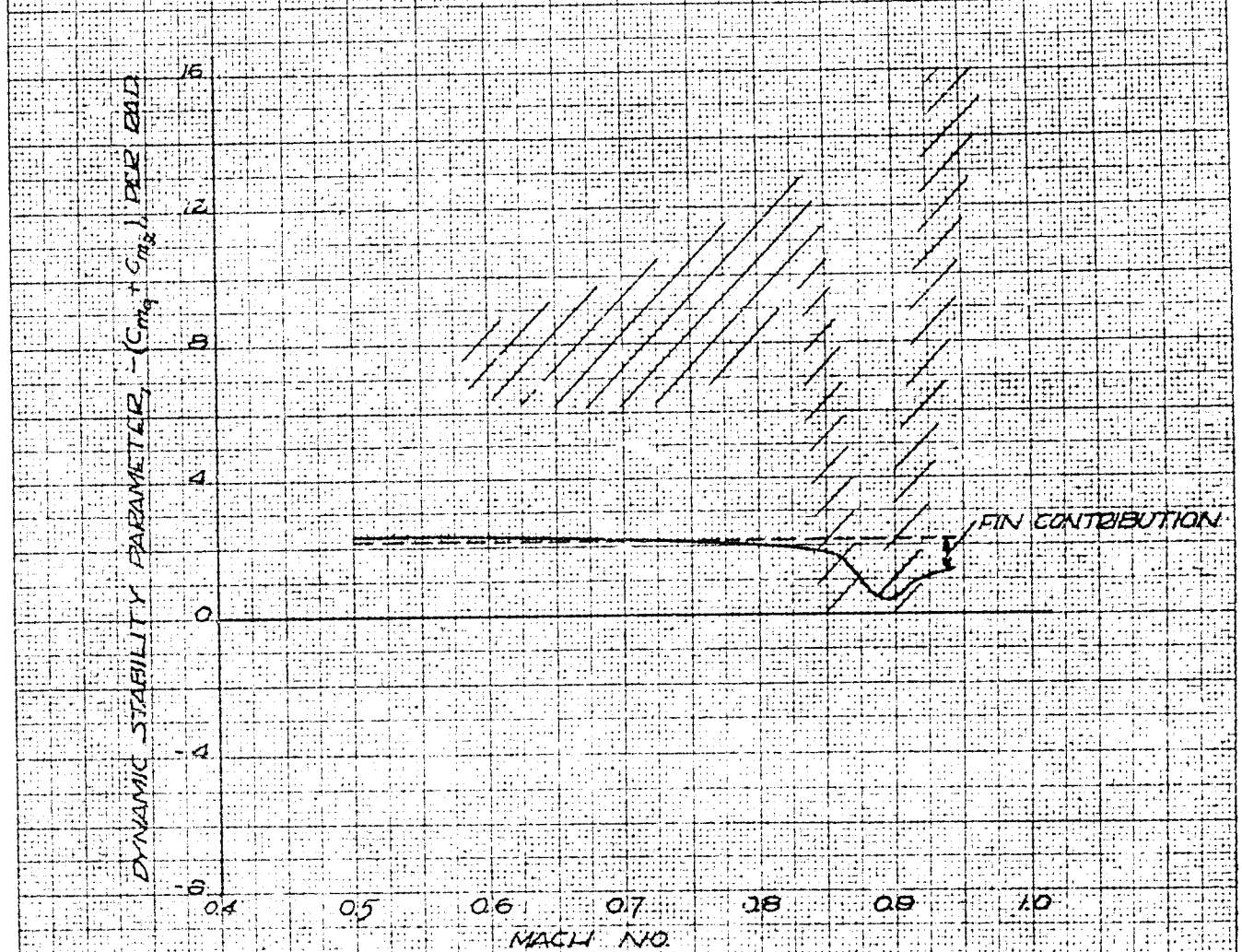


FIG. 6 - COMPARISON OF MK-6 DYNAMIC STABILITY PARAMETERS

[redacted]

UNCLASSIFIED

PREP. BY _____ DATE _____

[redacted]

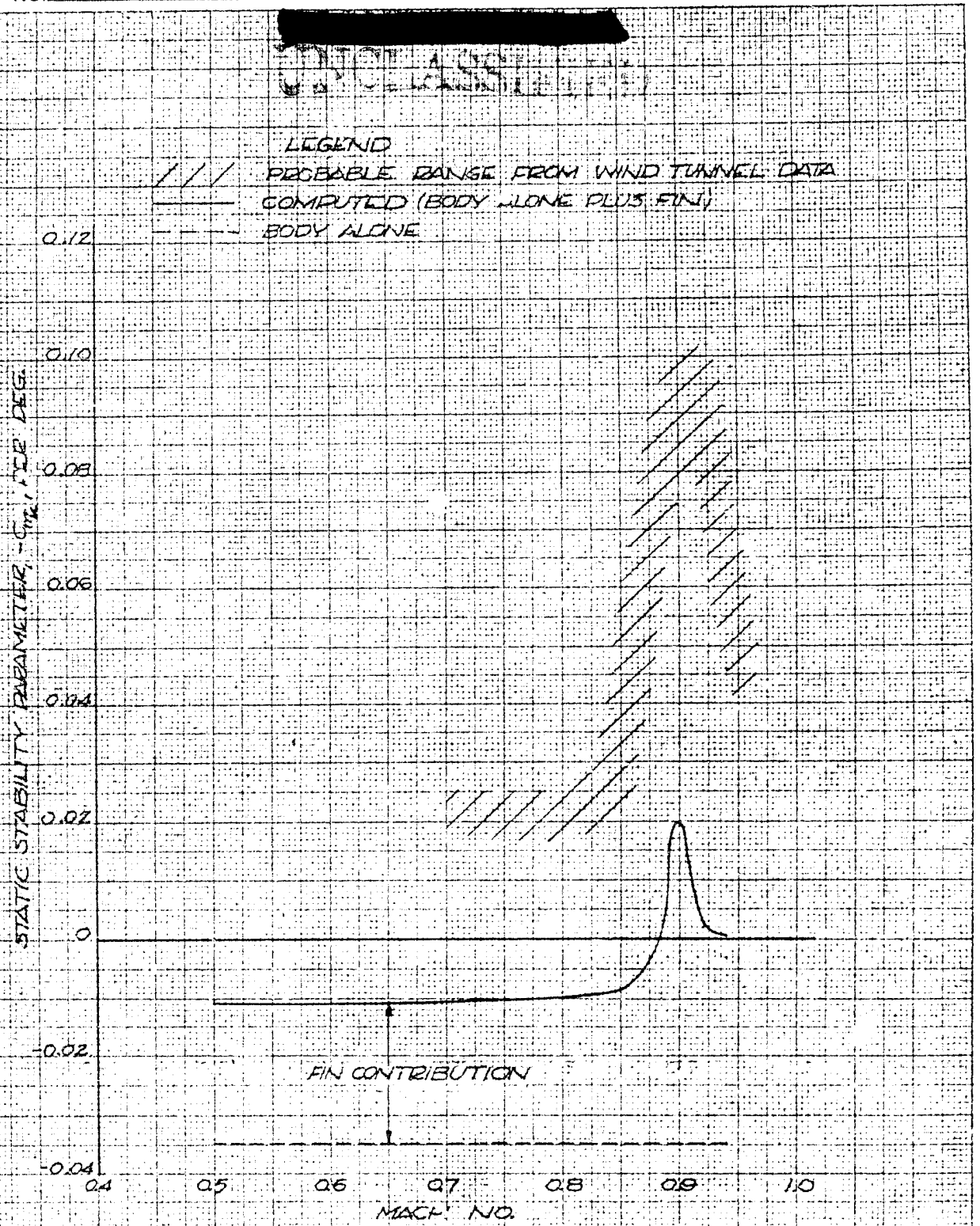


FIG 7 - COMPARISON OF MK-4 STATIC STABILITY PARAMETERS

[redacted]

[redacted]

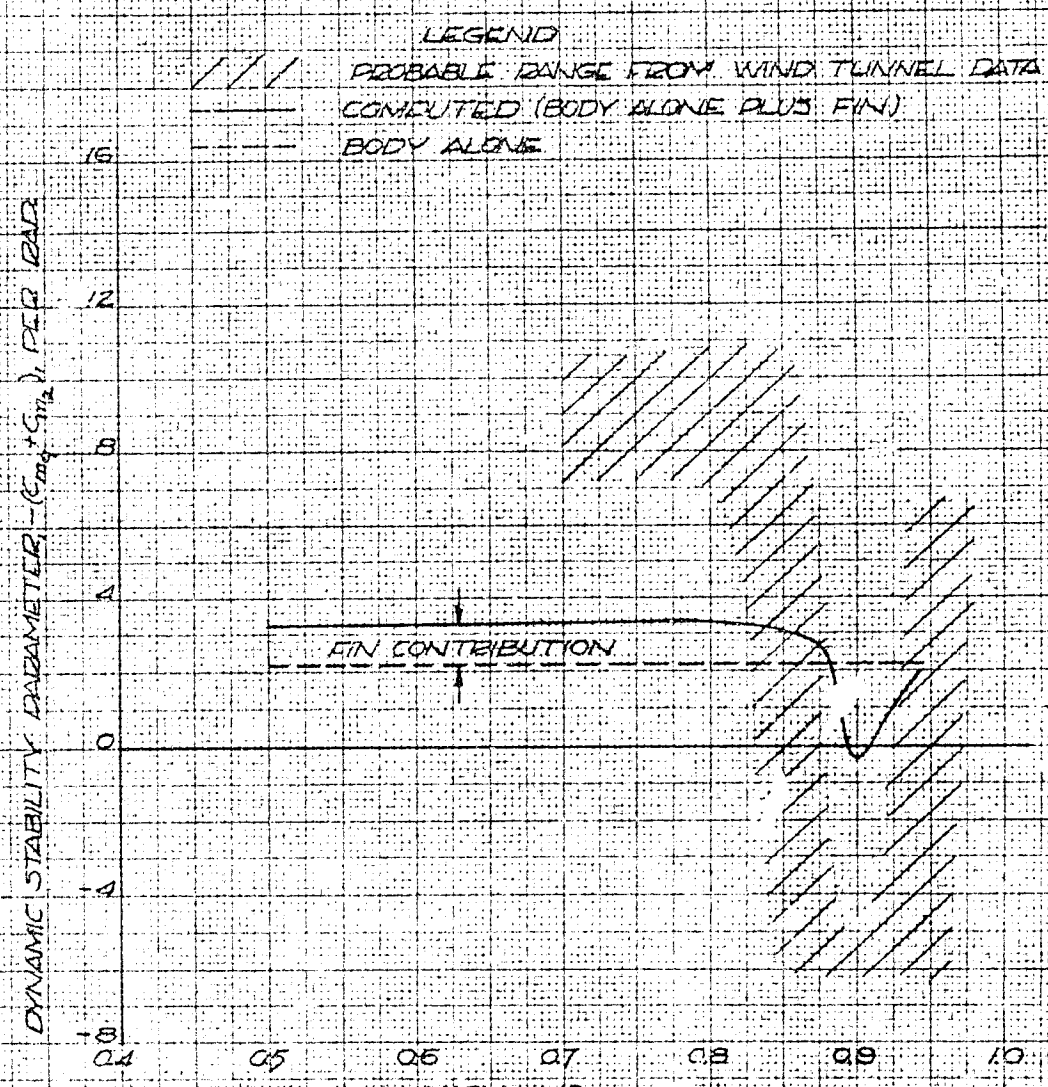


FIG 8 -COMPARISON OF MK-4 DYNAMIC STABILITY PARAMETERS

[redacted]



UNCLASSIFIED

[redacted]

UNCLASSIFIED

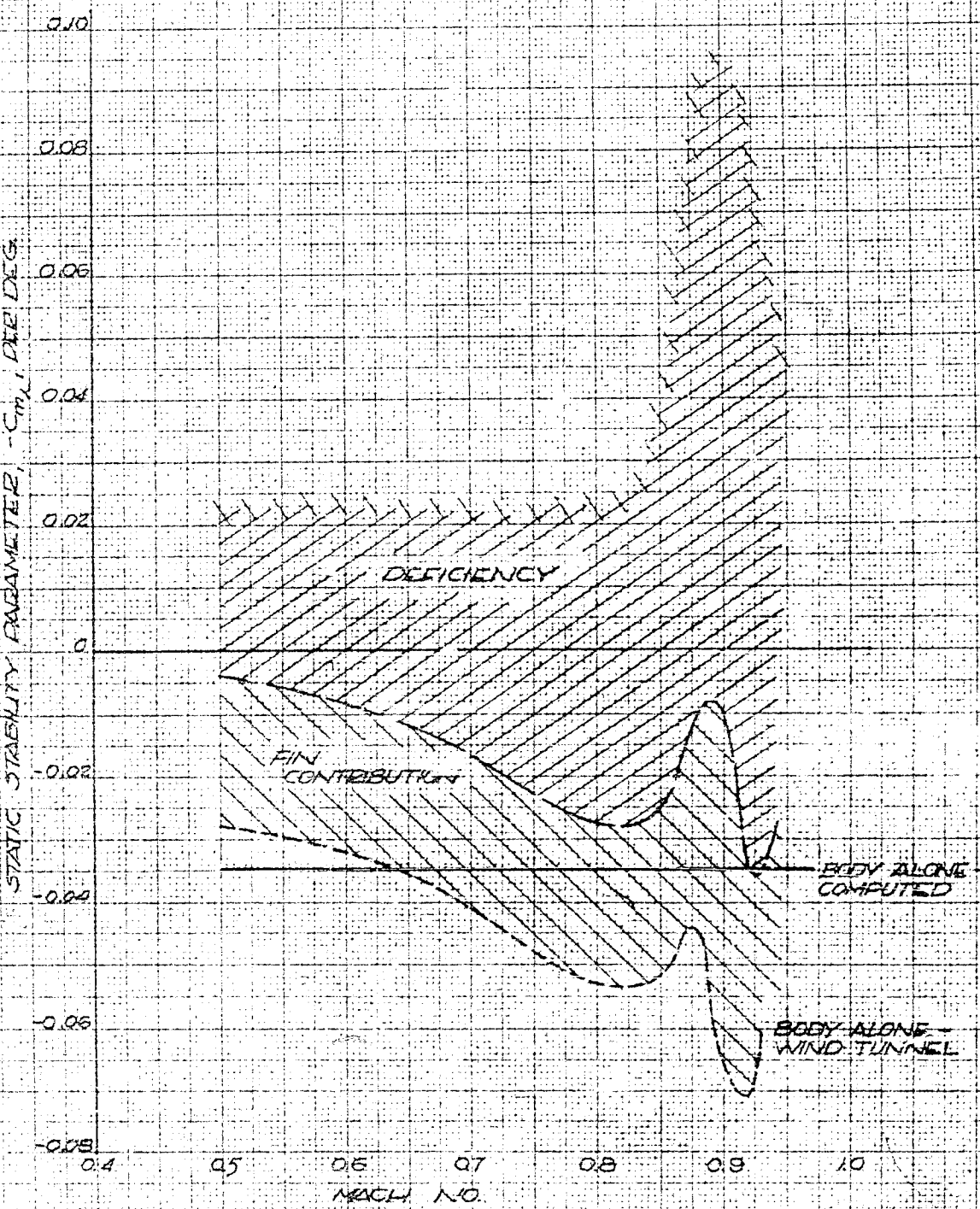


FIG 9 - BREAKDOWN OF MK-4 STATIC STABILITY PARAMETER

[redacted]



UNCLASSIFIED

[redacted]

UNCLASSIFIED

values of the body-alone static stability parameter, there results the curve shown in Fig. 9. The deficiency in the computed value of the parameter still remains. The only remaining contribution which has not been considered to this point, is the effect of the fin upon the body contribution. This being the case, the following analysis was evolved to attempt computation of this contribution.

Stability Contribution Due to Interference of the Fin with the Body

It would appear, if one examines the flow over a finned and finless body, that the flow patterns would be least similar in the region of the fins. On this basis, the following analysis evolved. In the previous section, the fins were assumed to lie in a plane normal to the pitch plane. If the body is at some angle of attack, $\alpha$, the flow normal to the axis of symmetry produces, for the finned configuration, pressures over the windward and leeward side of the afterbody quite different from those which would exist were the fins not there. In particular, with the fins on the body, the leeward side of the afterbody would most likely be in a separated cross flow region. If the local angle of attack in the afterbody region is $\alpha_a$, the cross flow potential for the finless body is, from Eq. (9)

$$\phi = - V\alpha_a\left(r + \frac{a^2}{r^2}\right)\cos\theta \tag{9}$$

and the pressure distribution around the afterbody at station x becomes:

$$p = p_a + \frac{1}{2}\rho V^2 \alpha_a^{\,2} (1 - 4 \sin^2 \theta) \tag{27}$$

Since the fins will modify this pressure distribution in the manner suggested, it seems reasonable to assume that $p$ for the windward side ($- 90 \leq \theta \leq 90^\circ$) is given directly by Eq. (27) and that the pressure on the leeward side ($- 90 > \theta > 90^\circ$) will be constant and equal to the value of $p$ from Eq. (27) at $\theta = \pm 90^\circ$. Actually, pressures over the windward and leeward side of the afterbody would probably be higher and lower, respectively, than those suggested above. However, Eq. (27) can be used to produce a term approximately proportional to the lift developed by the afterbody and then modified empirically to provide a better estimate. The pressure distribution given by Eq. (27) with the proper limits, i.e., $p$ for $- 90^\circ > \theta > 90^\circ$ equals $p$ at $90^\circ$, will yield a force on the afterbody, $f_x$, of magnitude (per unit length)

$$f_x = 2 \int_0^{\pi} p\, a \cos\theta \, d\theta \tag{28}$$

which, upon substitution of Eq. (27), becomes

$$f_x = 2a\left\{\int_0^{\pi/2}\left[\frac{1}{2}\rho V^2 \alpha_a^2 (1 - 4 \sin^2 \theta) + p_a\right] \cos\theta \, d\theta + \int_{\pi/2}^{\pi}\left[- 3\alpha_a^2 \left(\frac{1}{2}\rho V^2\right) + p_a\right] \cos\theta \, d\theta\right\} \tag{29}$$

Performing the indicated integration and evaluating at the limits yields

$$f_x = \frac{16}{3} a\, \alpha_a^2 \left(\frac{1}{2} \rho V^2\right) \tag{30}$$

[redacted]



UNCLASSIFIED

Now, by definition,

$$C_L]_a = \frac{f_x \ell_a}{\frac{1}{2}\rho V^2 S} = \frac{16}{3} \alpha_a^2 \frac{\bar{a}\, \ell_a}{S} \tag{31}$$

where

$\bar{a}$ = Mean radius of that portion of the afterbody between the leading and trailing edge of the fins.

The effect of the fins on the pressure distribution as illustrated in Fig. 10*, will increase the value of $C_L]_a$ given by Eq. (31) by a factor, K. Consequently Eq. (31) will be rewritten as:

$$C_L]_a = \frac{16K}{3} \alpha_a^2 \frac{\bar{a}\, \ell_a}{S} \tag{32}$$

where

K = Correction factor as noted above.

Since

$$C_m]_a = - C_L]_a \frac{\ell_{ta}}{d} \tag{33}$$

then

$$C_m]_a = - \frac{16K}{3} \alpha_a^2 \frac{\bar{a}\, \ell_a\, \ell_{ta}}{Sd} \tag{34}$$

It remains at this point to determine the value of the angle of attack of the afterbody, $\alpha_a$. In the ideal body case illustrated in Fig. 2(a), it is shown that $\alpha = \alpha_a$. However, in the actual case (Fig. 2(b)), it is shown that the angle of attack of the afterbody, $\alpha_a$, is not equal to the angle of attack of the body. Fortunately, it is possible to relate $\alpha_a$ to $\alpha$ in the following manner. From an earlier discussion of the downwash at the tail, it was shown that the local angle of attack at the fin base ($\theta = 90^\circ, 270^\circ$), was related to the angle of attack of the body for the ideal case by

$$\alpha_\ell = 2\alpha \tag{13}$$

There is no reason to expect this relation to vary significantly for the actual case if $\alpha$ is replaced by $\alpha_a$, i.e., the relation between the angle of attack at the tail and the angle of attack of the afterbody can be written:

$$\alpha_t\Big]_{\substack{r=a \\ \theta=90^\circ}} = 2\alpha_a \tag{35}$$

where $\alpha_t$ in (35) is evaluated at the root chord of the fin. Now, by definition, the root chord tail angle of attack, $\alpha_t\Big]_{\substack{r=a \\ \theta=90^\circ}}$, can be written, neglecting for the moment the effect of a pitching velocity,

$$\alpha_t\Big]_{\substack{r=a \\ \theta=90^\circ}} = \alpha - \epsilon_1 \tag{21}$$

---

* See also p. 102, "Aerodynamic Drag", by S. F. Hoerner, The Otterbein Press, 1951.

[redacted]

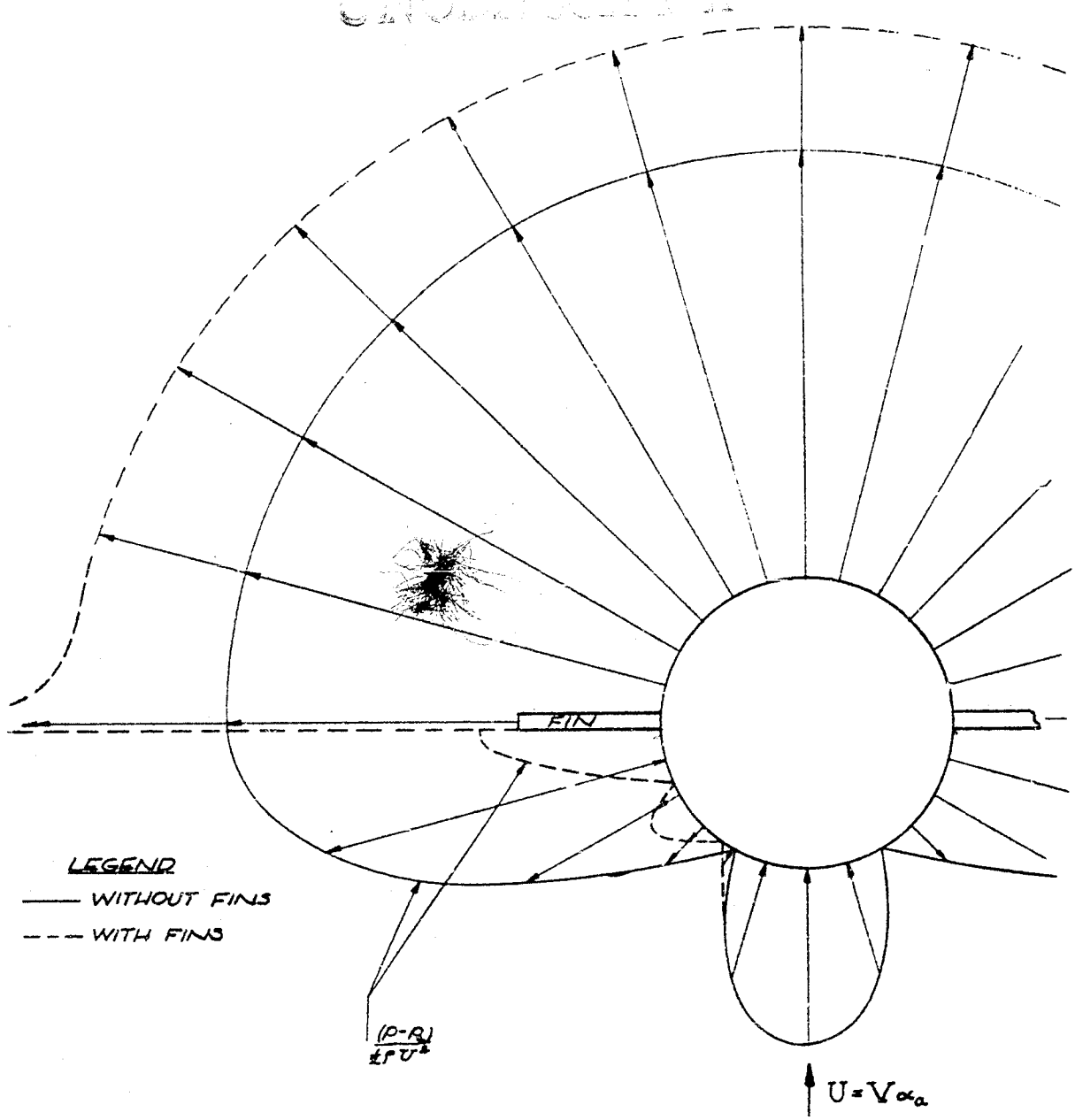


Fig. 10 - Effect of Fins on the Pressure Distribution due to Crossflow

and if $\epsilon$ is assumed to vary from root to tip of the fin in the ideal manner, though not necessarily having the ideal value, then from Eq. (18)

$$\frac{\epsilon_1}{\epsilon_2} = \frac{b^2}{a^2}$$

[redacted]

[redacted]

and (17)

$$\epsilon = \frac{\epsilon_1 + \epsilon_2}{2}$$

so that

$$\epsilon_1 = \frac{2\epsilon}{1 + \frac{a^2}{b^2}} \tag{36}$$

hence

$$\alpha_t\Big]_{\substack{r=a \\ \theta=90^\circ}} = \alpha - \frac{2\epsilon}{1 + \frac{a^2}{b^2}} = 2\alpha_a$$

so that

$$\alpha_a = \frac{\alpha}{2} - \frac{\epsilon}{1 + \frac{a^2}{b^2}} \tag{37}$$

Rewriting Eq. (37) to include the variation in $\epsilon$ with $\alpha$ and $t$ from Eq. (22) and taking into account the contribution of $q$ to $\alpha_a$ yields:

$$\alpha_a = \frac{\alpha}{2} - \frac{\frac{d\epsilon}{d\alpha}(\alpha - \dot{\alpha}\,\ell_{ta}/V)}{1 + a^2/b^2} + \frac{q\,\ell_t}{V} \tag{39}$$

where the lag in $\epsilon$ was assumed, as before, to originate at the body center of gravity. Substituting Eq. (38) into Eq. (34) and taking derivatives with respect to $\alpha$, $\dot{\alpha}d/2V$, $qd/2V$, and assuming $K$ is invariant with respect to these independent variables, yields for the afterbody contribution to stability:

$$-C_{m_q}\Big]_a = \frac{32K}{171.9}\left[\frac{\alpha}{2} - \frac{\frac{d\epsilon}{d\alpha}(\alpha - \dot{\alpha}\,\ell_{ta}/V)}{1 + a^2/b^2} + \frac{q\,\ell_{ta}}{V}\right]\left(\frac{1}{2} - \frac{d\epsilon/d\alpha}{1 + a^2/b^2}\right)\frac{\bar{a}\,\ell_a\,\ell_{ta}}{Sd} \tag{38}$$

$$-\left(C_{m_q} + C_{m_\alpha}\right)\Big]_a = \frac{64K}{3}\left[\frac{\alpha}{2} - \frac{\frac{d\epsilon}{d\alpha}(\alpha - \dot{\alpha}\,\ell_{ta}/V)}{1 + a^2/b^2} + \frac{q\,\ell_{ta}}{V}\right]\left(1 + \frac{d\epsilon/d\alpha}{1 + a^2/b^2}\right)\left(\frac{\ell_{ta}}{d}\right)^2 \frac{\bar{a}\,\ell_a}{S} \tag{39}$$

Equations (38) and (39) show that the afterbody contributions to stability possess some interesting characteristics. First, since $d\epsilon/d\alpha$ enters here in a manner similar to its entry in the fin contribution, the afterbody also possesses a "conservation of stability" characteristic. Secondly, the afterbody contribution is nonlinear, being dependent upon $\alpha$, $\dot{\alpha}$ and $q$; a characteristic which did not appear in the other contributions. This nonlinearity is, of course,

[redacted]



UNCLASSIFIED

[redacted]

UNCLASSIFIED

a result of the assumption of separated flow on the leeward side of the afterbody between the fins, and indicates that flow separation begets nonlinearities, a not unexpected conclusion. Equations (38) and (39) also indicate that in comparing model and prototype stability, the parameters should be compared only at values of $\alpha$, $\dot{\alpha}\ell_{ta}/V$ and $q\ell_{ta}/V$ which are equal for both the model and prototype. Reynolds and Mach numbers cannot be disregarded, of course.

Equations (38) and (39) were used to compute the afterbody contributions of the Mk 4 and Mk 6, with the afterbody constants taken as follows:

$\bar{a}$ = 1.92 ft (body radius at the 1/4 chord point on the fin root chord)

$\ell_a$ = 3.08 ft (length of the afterbody between the leading and trailing edges of the fin at the root chord)

$b$ = 3.34 ft

$\ell_{ta} = \ell_i$

The values of $d\epsilon/d\alpha$ were obtained from Fig. 4. To reduce the magnitude of the computations, the afterbody contributions were computed for the following, taken to be average, values:

$\alpha$ = 0.07 rad ($4^\circ$)

$\frac{\dot{\alpha}\ell_{ta}}{V} = \frac{q\,\ell_{ta}}{V}$ = 0.003 rad (corresponds to a maximum amplitude of oscillation of $6^\circ$, and a frequency of 2 cps at a velocity, V, of 1000 fps with correspondingly lower frequencies at lower velocities)

Preliminary computations indicated that the value of K should be taken as approximately five (5) to account for the higher than assumed pressures on the windward side of the afterbody, lower pressures on the leeward side, and the fact that the fin interference probably affects more of the afterbody than just that portion contained between the fin leading and trailing edges.

Since Eqs. (38) and (39) include the stability contribution of the afterbody alone <u>and</u> the fin interference effects, the body alone contributions must be revised to omit the afterbody contribution. This was done using Eqs. (4) and (7) assuming the body terminated at the position assumed to be the leading edge of the afterbody, i.e., the station at which the fin leading edge intercepts the body. The revised "body-alone-less-afterbody" constants then became:

$B_b$ = 13.85 ft$^2$ (was 5.94 ft$^2$)

$\ell - x_o$ = 4.25 ft (was 7.33 ft)

$B_m\ell$ = 121 ft$^3$ (was 156.7 ft$^3$)

The sum of the body-alone, afterbody, and fin contributions computed as indicated above are shown in Figs. 11 and 12 for the Mk 4 configuration. The agreement between the computed and wind-tunnel values of the stability parameters is excellent, considering the crudeness of the assumptions underlying the computation. Agreement of the Mk 6 values was poor, however, and the theory was examined to see if reasons existed for the poor correlation. A basic portion of the afterbody theory is dependent upon the value of $d\epsilon_1/d\alpha$ evaluated at the body surface from averaged values of $d\epsilon/d\alpha$ obtained from experimental measurements on the fin. The computations indicated that if the actual value of $d\epsilon_1/d\alpha$ were less negative than the value predicted from the theory, the agreement could be bettered. Since the extent of the separated wake over the Mk 6 is large, the predicted values of $d\epsilon_1/d\alpha$ on the afterbody could well have been too large negatively, since, in the case of separated flow, the maximum value of $d\epsilon/d\alpha$ could be expected to occur at a point outboard from the afterbody rather than at the afterbody surface as

[redacted]



UNCLASSIFIED

[redacted]

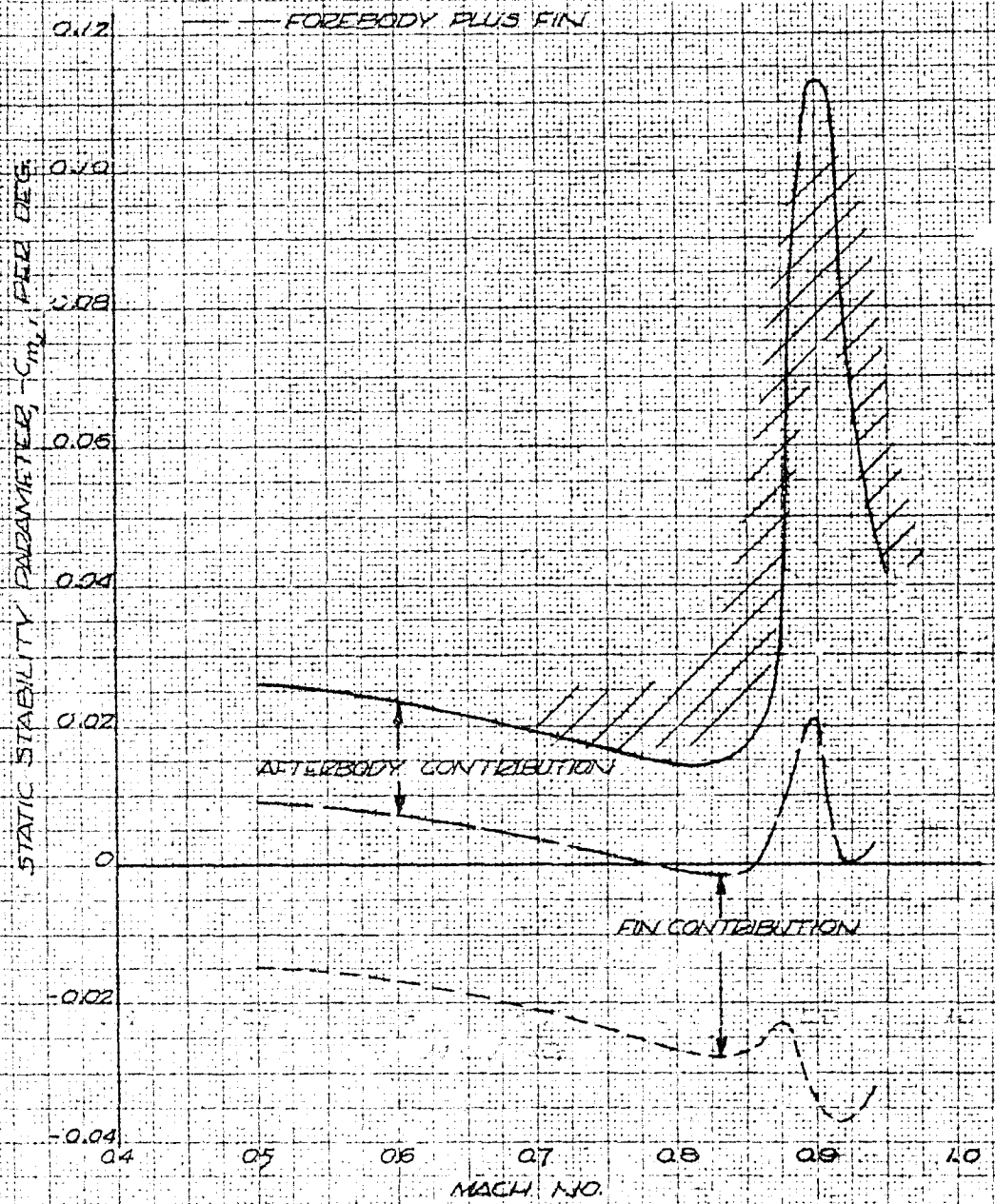


FIG 11 - COMPARISON OF MK-4 STATIC STABILITY PARAMETERS

[redacted]



UNCLASSIFIED

10 X 10 TO THE CM. 359-14

[redacted]

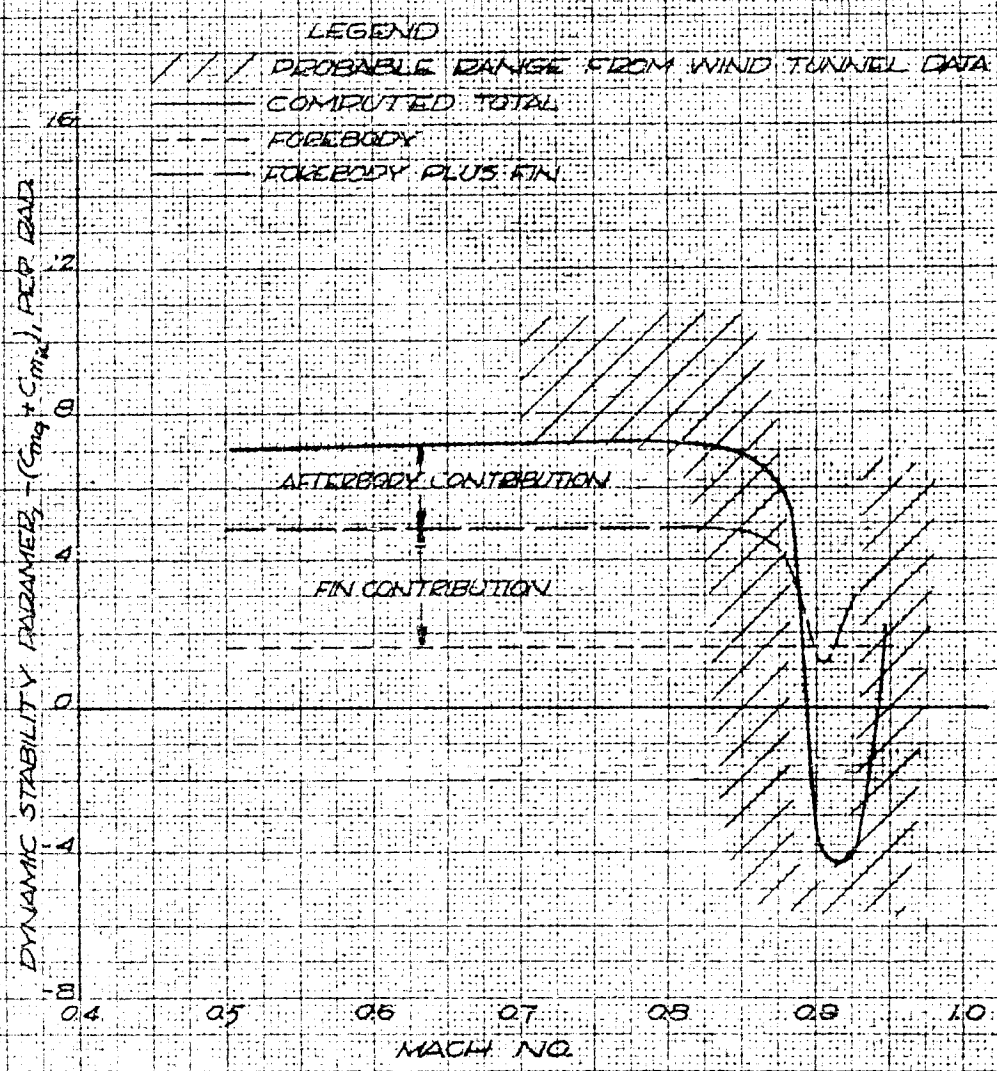


FIG 12 - COMPARISON OF MK-4 DYNAMIC STABILITY PARAMETERS

[redacted]

UNCLASSIFIED

predicted by Eq. (36), since the cross flow will have to diffuse through the wake. If the wake is large, the effective shape of the afterbody presented to the cross flow would be possibly blunter than a circle. This would increase the cross flow velocity at $\theta = 90^\circ$ and $270^\circ$ and increase $d\epsilon/d\alpha$ at the wake edge and the effective $d\epsilon/d\alpha$ over the fin. These effects are illustrated schematically in Fig. 13. An examination of the computed values in comparison with

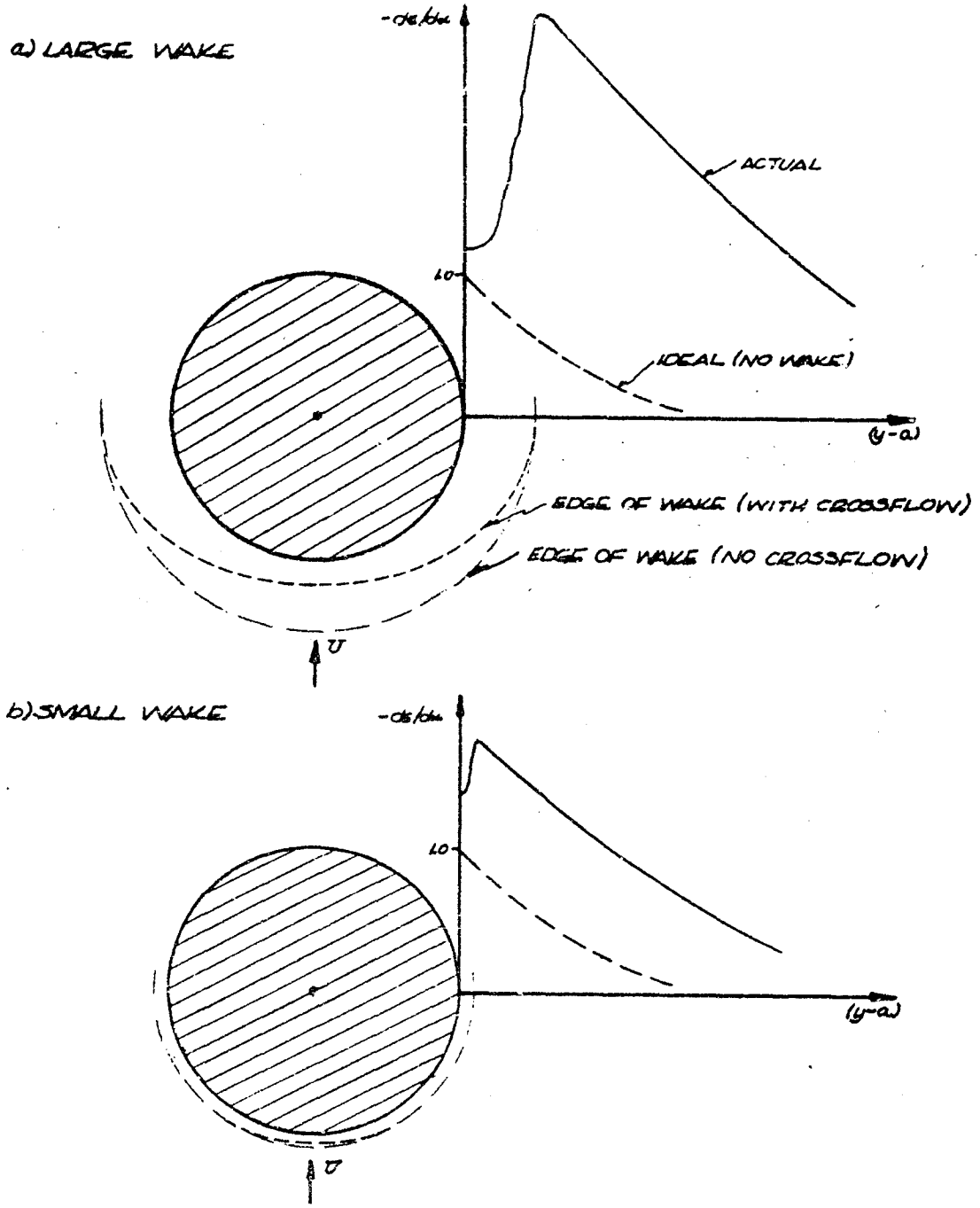


Fig. 13 - Possible Effect of Wake Size Upon Spanwise Variation of Downwash



[redacted]
UNCLASSIFIED

[redacted]

UNCLASSIFIED

the wind-tunnel values of the stability parameters indicated that $d\epsilon_1/d\alpha$ for the Mk 6 should be reduced by a factor of two (2). A recomputation made upon this basis resulted in the curves shown in Figs. 14 and 15. Figure 14 shows good correlation between computed and wind-tunnel values of the static stability parameter, but Fig. 15 indicates poor quantitative agreement of the dynamic stability parameters. However, the large separated wake could be responsible for more than the change in $d\epsilon_1/d\alpha$. One suspects that the lag in downwash in the wake may be quite different than the lag exterior to the wake, and the value in the wake may well be smaller than the value of lag exterior thereto. If the lag were smaller than that assumed for either portion of the wake, the computed dynamic stability parameter would increase. Lag does not affect the static stability parameter, however, so the above is a possible explanation for the poor correlation of dynamic stability parameters for the Mk 6. Because of the implicit nature of the lag term, no further attempts were made to better the dynamic stability parameters for the Mk 6, since further experimental data is necessary to intelligently evaluate the possibilities outlined above.

[redacted]



UNCLASSIFIED

[redacted]

UNCLASSIFIED

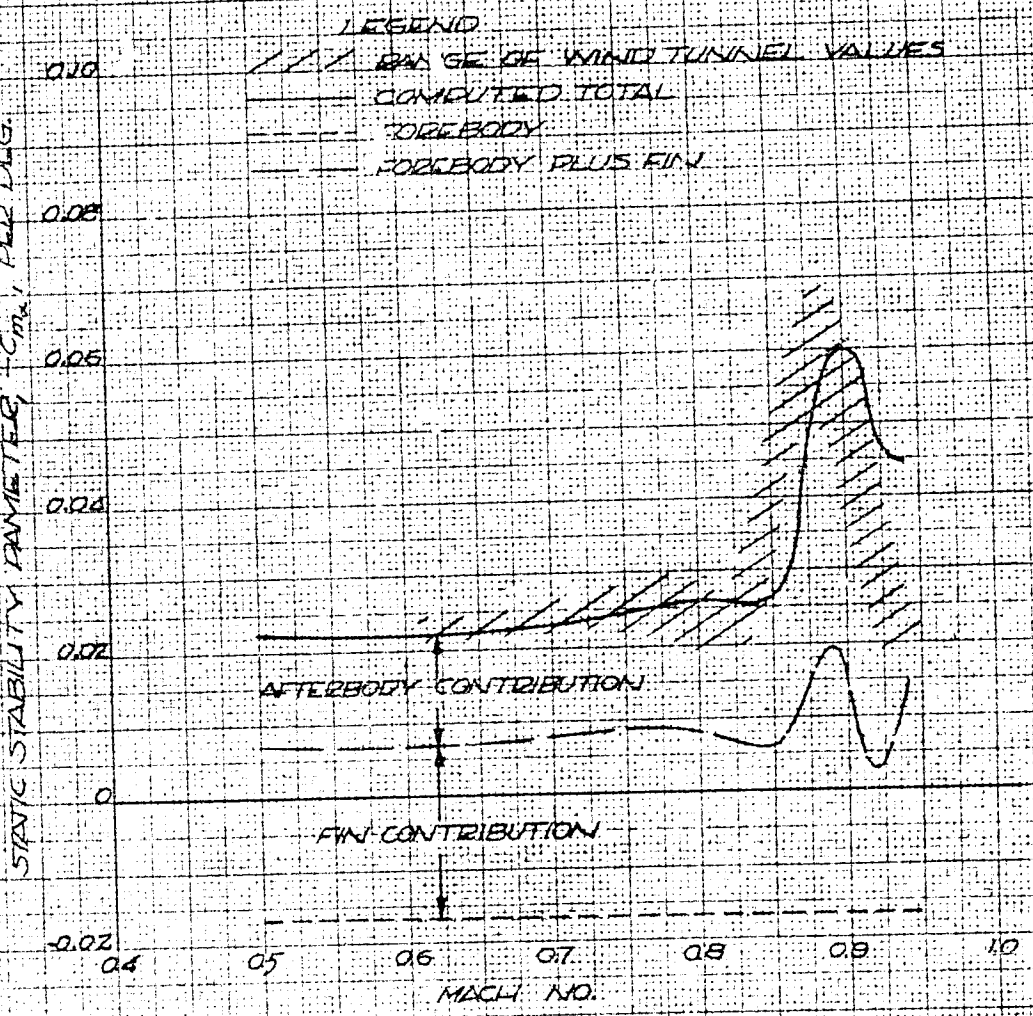


FIG. 14 - COMPARISON OF MK-6 STATIC STABILITY PARAMETERS

[redacted]

PREP. BY _____ DATE _____

UNCLASSIFIED

K&E 10 X 10 TO THE CM. 359-14 KEUFFEL & ESSER CO.

[redacted]

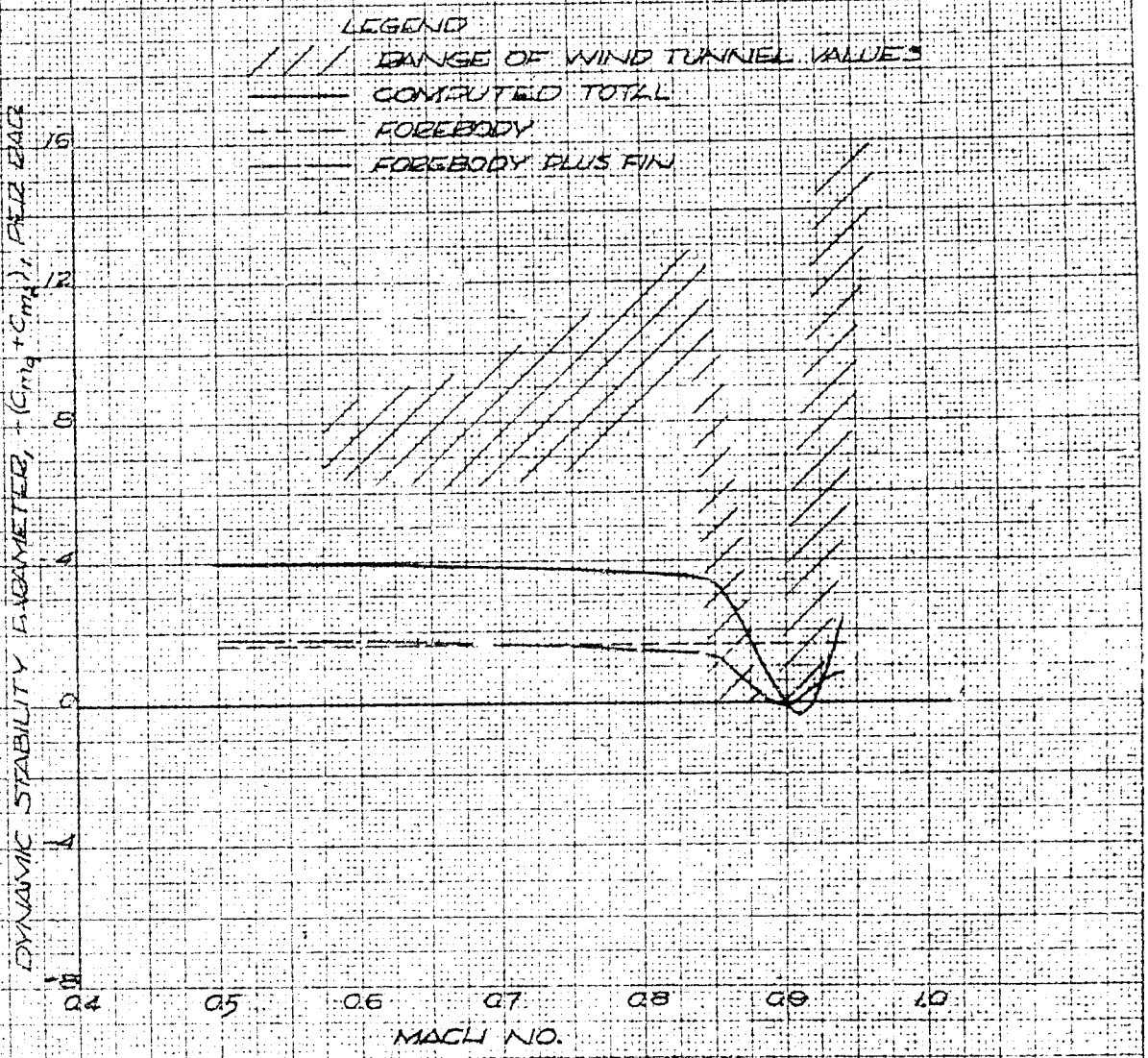


FIG 15 - COMPARISON OF MK-6 DYNAMIC STABILITY PARAMETERS

[redacted]

PREP. BY _____ DATE _____

UNCLASSIFIED

10 X 10 TO THE CM. 359-14

[redacted]

UNCLASSIFIED

## CONCLUSIONS

The foregoing analysis has compiled a reasonably complete picture of phenomena possibly contributing to the stability of fin-stabilized, low-fineness-ratio bodies of revolution. The analysis has indicated causes for the phenomena of stability conservation and nonlinear stability characteristics. In addition it appears possible to compute the stability characteristics of low-fineness-ratio shapes if the fin-lift-curve slope, downwash field, and lag in downwash are known. That the analysis contrived herein could achieve this modicum of success is somewhat remarkable, considering the crude assumptions which were made in its evolution. Actually, of course, the success of the analysis may be quite coincidental, since data does not exist which allows comparisons similar to those made for the Mk 4 and Mk 6 for other low-fineness-ratio shapes.

Even if the analysis is considered a success in the gross sense, the subtleties of the stability characteristics determined by this analysis are not retained. As an example, the analysis does not differentiate implicitly the change in stability accruing from the addition of bands to the Mk 4 to make the Mk 4 a Mk 6. The analysis does not allow prediction of stability using only the body geometry since it makes no attempt to predict values of fin-lift-curve slope, downwash field, and downwash lag nor the variation of these with Mach and Reynolds numbers, and as such, to achieve the prediction capability, further work is indicated. Possibilities of attaining this goal are discussed in the concluding section of this memorandum.

## RECOMMENDATIONS

As indicated in the preceding sections, although it is presently possible to compute the stability of low-fineness-ratio shapes, it is impossible under the circumstances to predict it. The moderate success achieved in the computations, however, indicates that prediction capabilities may be attained. To accomplish this end, several lines of attack are possible.

One obvious line of attack, based upon the degree of success achieved with the computational analysis presented herein, would be refinement of this analysis. It appears possible to include, for example, certain effects of viscosity and Mach number on the body and afterbody contributions, and to predict downwash. It also appears possible to compute the lag in downwash. Other types of analytical methods of attack are also possible, and an independent analysis is being completed by Lieber*. Since it appears feasible to pursue the above refinements and alternate analyses, it is suggested that these be actively continued.

The measure of success of any analysis cannot be determined, however, unless the analysis can be compared with specific data. Moreover, the rapidity with which a valid analysis can evolve is oftentimes a function of the type and kind of experimental verification available. It appears, then, that the capability of predicting stability characteristics of low-fineness-ratio bodies can best be attained by combining the analytical process with a concurrent experimental program; each designed to complement each other.

Currently, the "state-of-the-art" is not sufficiently well defined to enable prescription of a complete, unvarying program to attain the stability prediction capability. However, it is believed that sufficient knowledge exists to indicate a starting point. As such, the following program appears reasonable. It has been shown that the body of a low-fineness-ratio configuration produces flow phenomena which make prediction of the stability of these shapes a problem. Specifically, the body by itself is usually statically unstable although dynamically stable. To provide the static stability, fins are used, but incorporating the fins does not conclude the problem. The fins will provide a contribution to the dynamic stability, but this contribution

* "Dynamic Instability at Transonic Speeds", by Paul Lieber, Consultant to Sandia Corporation, to be published.

[redacted]



UNCLASSIFIED

is influenced by the body-produced flow field in which they are required to operate and in addition provide changes themselves in the flow field around the body. The lack of body-alone data makes it difficult to ascertain the body alone and mutual interference effects, and since the body is responsible for the stability problem it would appear reasonable to examine the body stability and induced flow field in more detail.

As a primary phase (Phase I), it is believed that an experimental program should be initiated to provide the following information:

1. The static and dynamic stability of the body alone.

2. The downwash and velocity field over the body.

3. The lag in downwash.

4. The effect of body shape parameters on items 1 through 3 above.

The results of this program will be used to check the body alone contribution to stability against the analysis, to refine the body-alone stability contribution prediction, and to initiate and confirm empirical and/or theoretical means of predicting downwash and downwash lag. To keep the program as simple as possible, it is suggested that body configuration changes be limited to nose flat area, and band numbers and location. Failing the above desires, the program would provide a signpost as to where next to proceed. It is anticipated that this program will result in one or more additional experiments to further investigate the effect of body shape changes on items 1, 2, and 3.

Phase II would then proceed with the effects of fins of various spans and chords upon:

1. Static and dynamic stability

2. The downwash field

3. The lag in downwash

4. The forces on the afterbody

5. The forces on the fins

Results from this Phase would aid refinements in the analysis of afterbody contribution, and induced effects of the fins on the body and vice versa. It is anticipated that various body shapes will be required in Phase II, and that these shapes will be suggested by the results of Phase I.

Additional experimental endeavor beyond this point will not be attempted. It would be hoped that Phase II would succeed in providing sufficient data to yield an analysis capable of stability prediction. It is to be emphasized, however, that Phases I and II may require amplification beyond the simple outline indicated. Eventually, it is anticipated that Reynolds number, oscillation frequency, and other parameters of nongeometric nature will require investigation beyond Phase II.

To recapitulate, the above suggestions are provided to attempt refinements in the analytical techniques of determining stability of low-fineness-ratio, fin-stabilized bodies of revolution. This is to occur through combined theoretical and experimental programs which will attempt to investigate the effects of geometric and nongeometric parameters, the actual deportment of the program being dictated by progress attained in two obvious preliminary phases.

To provide the most information for a minimum cost, it is suggested that existing models, rigs, and instrumentation be used where possible. In addition, the Mach number range desired need not extend beyond 0.95, since most of the significant variations in stability characteristics will occur at Mach numbers below this value.

[redacted]

UNCLASSIFIED

Some of the experimental data may be obtained using existing instrumentation. However, methods should be developed which will allow dynamic testing of unstable bodies, variation of the frequency of oscillations of a configuration, indication of instantaneous values of downwash at various points in the vicinity of the body, instantaneous forces on fins, and indication of surface pressures on the body during oscillation of the body. It is recommended that these developments begin as soon as possible.

## SUMMARY

The stability of fin-stabilized, low-fineness-ratio bodies of revolution has been crudely investigated as a function of body geometric shape, downwash characteristics, and fin lift. It has been shown that the stability characteristics of these shapes can be computed approximately if the downwash characteristics and fin lift are known, and that prediction of stability characteristics will require refined analytical methods of determining them. To provide an analytical method of determining stability an experimental program is suggested to allow development of a more rigorous theoretical method.

PAUL W. ROWE - 5141

Case No. 409.04
June 30, 1955

[redacted]

UNCLASSIFIED